Korean J. Chem. Eng., 34(2), 454-462 (2017)
DOI: 10.1007/s11814-016-0274-4

pISSN: 0256-1115
eISSN: 1975-7220

Optimization of fluoride adsorption onto natural and modified pumice using response surface methodology: Isotherm, kinetic and thermodynamic studies

Mohammad Hadi Dehghani[*,,†], Maryam Faraji[*,****,†], Amir Mohammadi[***], and Hossein Kamani[****]**

*Department of Environmental Health Engineering, School of Public Health,
Tehran University of Medical Sciences, Tehran, Iran
**Center for Solid Waste Research, Institute for Environmental Research,
Tehran University of Medical Sciences, Tehran, Iran
***Department of Environmental Health Engineering, School of Public Health,
Shahid Sadoughi University of Medical Sciences, Yazd, Iran
****Health Promotion Research Center, Zahedan University of Medical Sciences, Zahedan, Iran
(*Received 4 July 2016 • accepted 4 October 2016*)

Abstract−Natural pumice (NP), $FeCl_3 \cdot 6H_2O$ modified pumice (FEMP) and hexadecyl trimethyl ammonium bromide (HDTM.Br) modified pumice (HMP) were used for fluoride adsorption. The effect of pH (3-11), initial concentration (2-15 mg/L), and adsorbent dosage (0.2-0.8 g/L) on the defluoridation was optimized by using central composite design (CCD) in the response surface methodology (RSM). Results showed optimum condition in the pH=3, initial concentration=2 mg/L, and adsorbent dosage=0.71, 0.75, 0.70 g/L with the maximum removal efficiency of 9.39, 76.45, and 95.09% for NP, FEMP, and HMP, respectively. The adsorption equilibrium and kinetic data was in good agreement with Freundlich and pseudo-second order reaction. Thermodynamic parameters indicated a non-spontaneous nature for NP and spontaneous nature for FEMP and HMP. Positive enthalpy illustrated the endothermic nature of the process. On the basis of results, modification of pumice led to an increase in the fluoride removal efficiency.

Keywords: Thermodynamic, Central Composite Design, Response Surface Methodology, Fluoride Adsorption, Pumice Modification

INTRODUCTION

Due to the abundance of fluorine in the earth's crust, fluoride compounds are usually found in groundwater [1]. The WHO has specified the tolerance limit of fluoride in drinking water as 1.5 mg/L. At low concentrations, it has beneficial effects on teeth and bones [2]. Depending on the concentration and the duration of uptake, excess intake of fluoride leads to various diseases such as osteoporosis, arthritis, brittle bones, brain damage, Alzheimer syndrome and mottling of the teeth [3]. In the areas with high minerals, well water may contain fluoride up to 10 mg/L and much higher concentration can sometimes be found.

Several methods have been used for the fluoride removal from water sources, including coagulation/chemical precipitation, reverse osmosis, ion exchange, nano-filtration, adsorption and electro coagulation [4-9]. Among these, adsorption is still one of the most extensively used methods. Zhang et al. revealed that layered double hydroxides (LDHs)/Al_2O_3 composites from waste paper fibers had high adsorption capacity for fluoride adsorption [10]. Also, natural compounds such as bauxite ore and charcoal could be easily used for defluoridation [11]. In another study, Zhang et al. reported that bentonite from group of clay minerals was economical compound for defluoridation [12].

Pumice is a low cost natural adsorbent which has been widely tested and used in water treatment as an adsorbent, filter bed, and support media [13]. This volcanic stone has a light appearance and a porous structure which is due to the release of gases during solidification. The main advantages of pumice in comparison with other natural or synthetic adsorbents are high adsorption capacity and lack of toxicity [14].

Response surface methodology (RSM) is a collection of mathematical and statistical techniques useful for developing, improving, and optimizing processes. RSM uses an experimental design such as the central composite design (CCD) to fit a model by the least squares technique [15,16]. The significance of the proposed model is then evaluated by using the diagnostic checking tests provided by the analysis of variance (ANOVA). In several studies, CCD is used to assess the results and efficiency of the process [17-21].

Since the investigation of fluoride adsorption using the CCD with RSM in the R software has not yet been reported, our aim was to study the optimum conditions of fluoride adsorption in an aqueous medium onto natural and modified Iranian pumice using the R software by the RSM package as alternative to the conventional methods. $FeCl_3 \cdot 6H_2O$ modified pumice was used as fluoride adsorbent for the first time in this study. We determined the optimum of pH, initial concentration, and adsorbent dosage on fluoride removal efficiency by RSM.

†To whom correspondence should be addressed.
E-mail: hdehghani@tums.ac.ir, m_faraji28@yahoo.com

MATERIALS AND METHODS

1. Preparation of Adsorbent

Natural pumice was obtained from the Tikmadash mine in the northwest of Iran. Initially, pumice was ground and then sieved to the required particle size fraction of 200-2,000 μm, which was later followed by washing several times with distilled water. To enhance the surface porosity and removal of impurities, pumice was rinsed in HCL solution 1 N for 48 h at room temperature and then washed with distilled water several times until effluent turbidity reached <1 NTU and solution pH was 7. Afterwards, pumice was dried at 105 °C for 8 h. The pretreated pumice (100 g, 200-2,000 μm) was exposed with $FeCl_3{\cdot}6H_2O$ (1 mol/L) at pH 8 for FEMP and hexadecyl trimethyl ammonium bromide (HDTM.Br) (2.5 mmol/L) at pH 10 for HMP. This suspension was shaken for 10 h at 220 RPM at room temperature. The suspension was then filtered, dried at 120 °C for 2.5 h, washed several times with distilled water, and dried at 120 °C for 6 h.

Natural pumice (NP), $FeCl_3{\cdot}6H_2O$ modified pumice (FEMP), and HDTM.Br modified pumice (HMP) were used in the present study. The chemicals were all analytical grade obtained from Merck Co (Germany).

2. Characterization of Adsorbents

The surface textural and morphological structure of the pumice was analyzed with a HITACHI Model S-4160 field emission scanning electron microscope (FESEM). The mean pore diameter, specific surface area, and pore volume were determined by the Brunauer-Emmett-Teller (BET) (nitrogen sorption isotherm) method, using a micrometrics particle size analyzer (Belsorp mini II, Japan). Modified adsorbent was analyzed by X-ray diffraction (XRD) and X-ray fluorescence (XRF) (Philips, Model XPERT PW 3040/60). The Fourier transform infrared spectroscopy (FTIR) study used the HP 6890. The pH of the zero point charge (pH_{ZPC}) was determined by a method reported elsewhere [22].

3. Experimental Design

The effects of independent variables on the dependent variable (fluoride removal efficiency) and the optimum conditions were investigated using the R software [23] by response surface methodology (RSM) package [24]. P-value less than 0.05 was considered significant in all statistical analyses.

The central composite design was used to investigate the effect of pH (x_1) (3-11), initial concentration (x_2) (2-15 mg/L), and adsorbent dosage (x_3) (0.2-0.8 g/L) on the defluoridation. The selection of variables was based on the previous studies.

The experimental method results were used to specify appropriate empirical equations (second-order polynomial multiple regression model, Eq. (1)):

$$Y=\beta_0+\beta_1X_1+\beta_2X_2+\beta_3X_3+\beta_{12}X_1X_2+\beta_{13}X_1X_3+\beta_{23}X_2X_3+\beta_{11}X_1^2+\beta_{22}X_2^2+\beta_{33}X_3^2 \quad (1)$$

The predicted response (Y) was therefore correlated to the set of regression coefficients (β): intercept (β_0), linear (β_1, β_2, β_3), interaction (β_{12}, β_{13}, β_{23}) and quadratic coefficients (β_{11}, β_{22}, β_{33}).

4. Batch Adsorption Studies

Batch fluoride adsorption studies on NP, FEMP, and HMP were conducted based on CCD in triplicates. The pH was adjusted by using H_2SO_4 or NaOH 1N. A stock solution of fluoride was made by dissolving NaF (2.21 g) in distilled water (1,000 mL). One-hundred milliliter fluoride solutions were agitated with different pH, initial concentrations, and adsorbent dosages at equilibrium time and room temperature by reciprocating shaker at 120 RPM. After that, the solutions were filtered (0.45 μm, Whatman filter paper) and then the residual fluoride concentration was analyzed at a maximum wavelength of 570 nm using UV/VIS spectrophotometer (Perkin-Elmer, Lambda 25) according to standard methods for the examination of water and wastewater [25].

The amount of adsorbed fluoride at equilibrium (q_e), and fluoride removal efficiency (Y) was calculated from the mass balance equation presented in Eqs. (2) and (3), respectively:

$$q_e=V/M\times(C_0-C_e) \quad (2)$$

$$Y(\%)=C_0-C_e/C_0\times100 \quad (3)$$

where C_e and C_0 are the equilibrium and the initial concentrations of fluoride (mg/L) respectively, q_e is equilibrium fluoride concentration on the adsorbent (mg/g), V is the volume of fluoride solution (L), M is the mass of adsorbents (g), and Y is the removal efficiency.

Apart from the correlation coefficient (R^2), the validity of the adsorption isotherm and kinetic models was assessed with Marquardt's percent standard deviation (MPSD) and the hybrid error functions (HYBRID), which can be described as Eqs. (4) and (5):

$$MSD=100\left[\frac{1}{N-P}\Sigma_{i=1}^{N}\left(\frac{q_{ei}^{exp}-q_{ei}^{cal}}{q_{ei}^{exp}}\right)^2\right]^{0.5} \quad (4)$$

$$HYBRID=(100/N-P)\Sigma_{i=1}^{N}\left[\frac{(q_{ei}^{exp}-q_{ei}^{cal})^2}{q_{ei}^{exp}}\right] \quad (5)$$

where in two equations, N is the observations in the experiments, P is the number of parameters in the regression model, q_{ei}^{exp} is the observation of the batch experiment i, and q_{ei}^{cal} is estimated from the equations for the corresponding q_{ei}^{exp}. The smaller MPSD and HYBRID values revealed more accurate estimations of values [22, 26].

5. Determining Optimal Settings

This method uses iterative numerical methods to estimate the optimal conditions, starting from initial speculations and making improvements until the optimal conditions found according to the constraints. The Solver utility in MS Excel (*solved add-in*) is a convenient way to do so. To set it up, we needed to enter the coefficients from the un-coded model. We also needed initial speculations (center points from the response surfaces are good start points). A value of the yield was then calculated using the regression equation. We then set up the solver to maximize efficiency by varying three variables subject to the constraints (3≤pH≤11, 2≤ Initial concentration ≤15, 0.2≤ adsorbent dosage ≤0.8).

RESULTS AND DISCUSSION

1. Adsorbent Characteristics

The FESEM micrographs of the natural and modified adsorbents that show surface morphology of the samples at a magnification of 600× are illustrated in Fig. 1. While the surface of natural

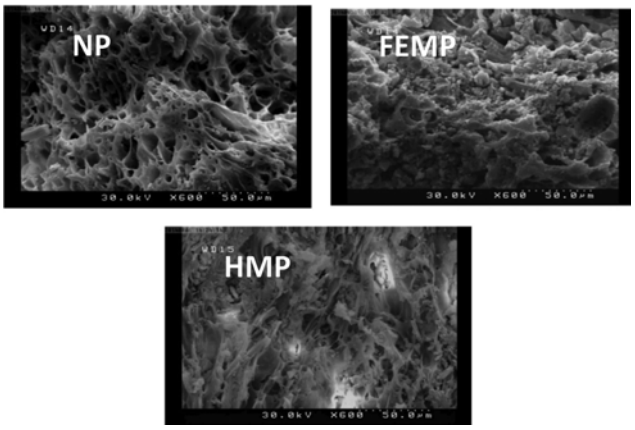

Fig. 1. SEM image of NP, FEMP and HMP.

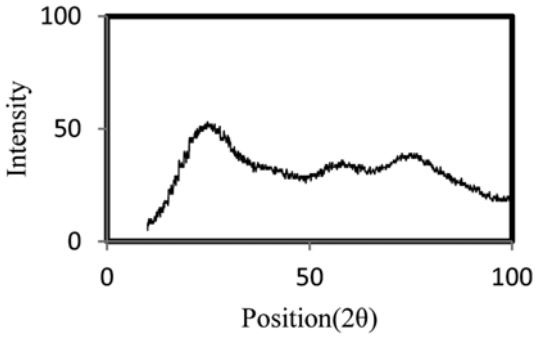

Fig. 2. The XRD pattern for NP.

pumice displayed texture with larger grains and sharper edges, the HMP and FEMP appeared smooth surfaces and smaller grains. The surface area increased in the following order: NP (9.5 m^2/g)< FEMP (24.5 m^2/g)<HMP (31.5 m^2/g). Results of the present study were in agreement with other studies conducted previously [27-29].

The XRF results of NP showed percent of components as SiO_2 (65.87), Al_2O_3 (15.32), CaO (4.21), Fe_2O_3 (3.42), K_2O (1.29), Na_2O (1.16), MgO (1.04), TiO_2 (0.56), Cl^- (0.49), P_2O_5 (0.37), SO_3 (0.17) and SrO (0.12). Various studies reported that the main component of pumice is SiO_2 [14,30,31]. The negative charge of the silicate and aluminum layers is an important factor in the adsorption of modifiers on the pumice surface and finally fluoride anion adsorption. The XRD pattern for NP is demonstrated in Fig. 2. SiO_2 is the main chemical component of pumice and since its amorphous phases cannot be specified by XRD, recognizable peaks and phases were not observed in the XRD result. This result is not in agreement with the findings of another study [29].

The specific surface area ($m^2\ g^{-1}$) that was calculated by the BET, average pore diameter (nm) and total pore volume ($cm^3\ g^{-1}$) of the adsorbents obtained from the desorption branch of nitrogen isotherm by the Barrett-Joyner-Halenda (BJH) method for NP, FEMP and HMP were (9.51, 18.39, 0.0437), (24.50, 7.11, 0.0435), and (31.51, 2.23, 0.0432), respectively. The amount of of SiO_2, Al_2O_3, and BET of the selected pumice in this study were different from other studies. These differences can be attributed to the geological structure of the pumice sources. The significant improvement of the surface area after modification can be attributed to the removal of components occupying the pores of the pumice, resulting in more accessible pores and therefore a larger surface area. This finding was in agreement with other studies [29,30,32]. The pore diameter of the adsorbent decreased after modification. The reason is covering the external surface of pumice by HDTMA and $FeCl_3$.

Fig. 3 represents FTIR spectra for adsorbents. The bands at 3,420-3,543 cm^{-1} belong to the stretching vibration of H_2O molecules [33]. The band around 1,638-1,645 cm^{-1} is associated with the stretching vibration of OH groups of water absorbed from the outside environment [34,35]. For Si-O and Al-O bonds, the characteristic stretching vibrations were studied at 1,035-1,045 cm^{-1} and the bending modes of groups were observed between 400 and 500 cm^{-1}. The Si-O-Al stretching vibration is recorded around 787-788 cm^{-1} [29]. The band at 2,800 cm^{-1} may be due to OH bending vibration [36].

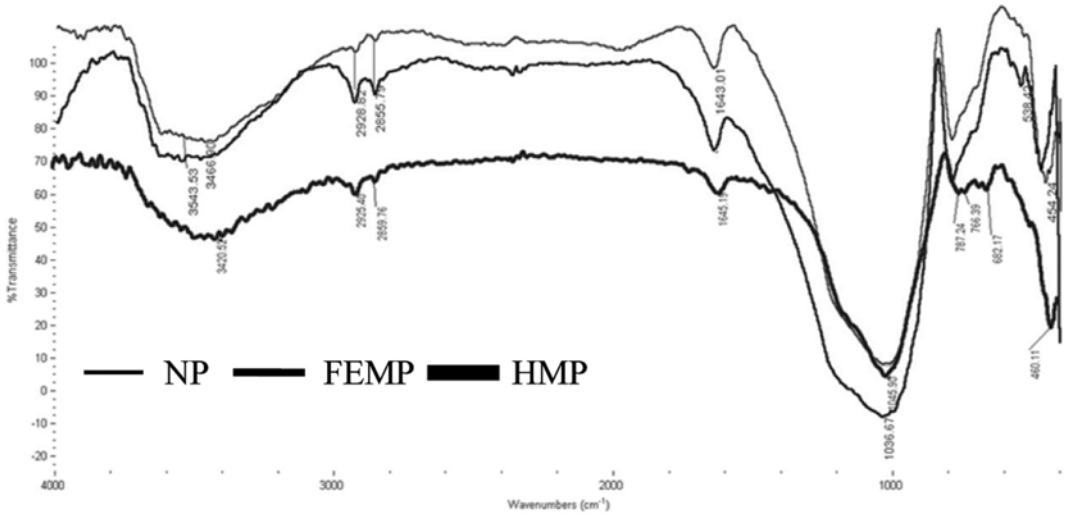

Fig. 3. FTIR spectrum.

Table 1. Central composite design and observed responses

Run	Actual factors			Removal (%)		
	pH	Initial concentration (mg/L)	Adsorbent dosage (g/L)	NP	HMP	FEMP
1	4.62	12.36	0.67	6.50	70.20	52.40
2	4.62	12.36	0.32	5.40	62.10	43.20
3	9.37	12.36	0.67	5.80	65.70	45.50
4	9.37	12.36	0.32	5.20	60.40	41.60
5	9.37	4.63	0.32	6.70	70.30	53.60
6	4.62	4.63	0.32	8.10	81.90	65.30
7	4.62	4.63	0.67	8.70	86.80	69.60
8	9.37	4.63	0.67	7.80	77.30	63.10
9	7.00	8.50	0.50	7.70	76.90	61.60
10	7.00	15.00	0.50	5.10	56.90	40.50
11	7.00	8.50	0.50	7.60	76.60	60.30
12	7.00	8.50	0.50	7.60	76.70	60.70
13	7.00	8.50	0.80	7.80	77.60	63.70
14	11.00	8.50	0.50	6.40	70.10	51.20
15	7.00	8.50	0.20	6.20	66.20	48.60
16	3.00	8.50	0.50	8.00	81.50	64.10
17	7.00	8.50	0.50	7.20	76.40	59.60
18	7.00	8.50	0.50	7.80	77.30	62.90
19	7.00	2.00	0.50	8.00	81.80	65.20
20	7.00	8.50	0.50	7.40	73.60	59.20

2. Central Composite Statistical Analysis

Experiments were performed based on CCD shown in Table 1 for the development of mathematical equations. Fluoride removal efficiency was assessed as a function of pH (x_1), initial concentration (x_2) and adsorbent dosage (x_3) and calculated as the sum of a constant, three first-order effects (x_1, x_2 and x_3), three interaction effects (x_1x_2, x_1x_3 and x_2x_3) and three second-order effects (x_1^2, x_2^2 and x_3^2).

Table 2. Results of the second-order model for fluoride adsorption by NP

Coefficients	Estimate	SE	t	p
(Intercept)	7.180	1.337	5.369	0.0003
pH	−0.089	0.198	−0.451	0.6610
Solute	−0.065	0.116	−0.561	0.5869
Adsorbent	7.708	2.675	2.881	0.0163
pH: Solute	0.020	0.009	2.272	0.0463
pH: Adsorbent	−0.009	0.220	−0.043	0.9659
Solute: Adsorbent	0.031	0.136	0.229	0.8230
pH^2	−0.018	0.011	−1.754	0.1099
$Solute^2$	−0.020	0.004	−4.872	0.0006
$Adsorbent^2$	−5.471	1.903	−2.874	0.0165
Multiple R-squared	0.976	Adjusted R-squared		0.955
Lack of fit	0.44	p-value		5.56E-07

Notes: Where SE=standard error, t=student test, p=probability

Table 3. Results of the second-order model for fluoride adsorption by FEMP

Coefficients	Estimate	SE	t	p
(Intercept)	55.185	11.044	4.996	0.0005
pH	−0.376	1.639	−0.229	0.8231
Solute	−0.411	0.961	−0.428	0.6778
Adsorbent	−65.166	22.095	2.949	0.0145
pH: Solute	0.140	0.073	1.901	0.0864
pH: Adsorbent	−0.067	1.818	−0.037	0.9713
Solute: Adsorbent	−0.045	1.128	−0.039	0.9690
pH^2	−0.163	0.088	−1.861	0.0923
$Solute^2$	−0.154	0.034	−4.550	0.0010
$Adsorbent^2$	−43.003	15.722	−2.735	0.0210
Multiple R-squared	0.977	Adjusted R-squared		0.956
Lack of fit	0.14	p-value		5.30E-07

Notes: Where SE=standard error, t=student test, p=probability

RSM used the special functions FO, TWI, PQ, or SO (for first-order, two-way interaction, pure quadratic and second-order). We first fit a first-order response-surface model to the data to obtain the regression equations and then an analysis by ANOVA to assess the goodness of fit. An insignificant lack of fit was desired (p-value> 0.05) because it showed that the model is valid. There was a significant lack of fit for the first-order model. We could add two-way interactions. There was still a small p-value for the lack of fit. We should fit a full second-order model [24]. Based on the Table 2-4, the lack of fit was insignificant in second-order model for NP, FEMP, and HMP equal to 0.44, 0.14, and 0.49, respectively. The insignificant lack of fit showed that the model was valid for the data.

Therefore, the second-order model was selected for further analysis. A second-order empirical model was fitted between the experimental results obtained on the basis of the central composite experimental design model and the input variables. The final equations obtained in terms of actual factors are given in the Eqs. (6)-(8):

Table 4. Results of the second-order model for fluoride adsorption by HMP

Coefficients	Estimate	SE	t	p
(Intercept)	86.655	7.991	10.844	7.53E-07
pH	−3.367	1.185	−2.840	0.0175
Solute	−1.268	0.696	−1.822	0.0983
Adsorbent	57.789	15.987	3.615	0.0047
pH: Solute	0.207	0.053	3.876	0.0030
pH: Adsorbent	−0.067	1.315	−0.051	0.9604
Solute: Adsorbent	0.204	0.817	0.250	0.8073
pH^2	0.015	0.063	0.237	0.8171
$Solute^2$	−0.126	0.024	−5.151	0.0004
$Adsorbent^2$	−41.626	11.376	−3.659	0.0044
Multiple R-squared	0.985	Adjusted R-squared		0.971
Lack of fit	0.49	p-value		6.50E-08

Notes: Where SE=standard error, t=student test, p=probability

$$Y_{NP}(\%)=7.18-0.09X_1-0.06X_2+7.71X_3-0.02X_1^2-0.02X_2^2-5.47X_3^2 +0.02X_1X_2-0.01X_1X_3+0.03X_2X_3 \quad (6)$$

$$Y_{FEMP}(\%)=55.18-0.37X_1-0.4X_2+65X_3-0.16X_1^2-0.15X_2^2-43X_3^2 +0.14X_1X_2-0.06X_1X_3-0.04X_2X_3 \quad (7)$$

$$Y_{HMP}(\%)=86.6-3.36X_1-1.27X_2+57.5X_3+0.01X_1^2-0.12X_2^2-41.6X_3^2 +0.21X_1X_2-0.06X_1X_3+0.2X_2X_3 \quad (8)$$

where X_1, X_2 and X_3 are pH, fluoride concentration, and adsorbent dosage, respectively. The correlation coefficient (R^2) of the models, >0.9, indicated a good fit between predicted values from the model and experimental data points. The p-values were used to check the significance of each coefficient. It can be seen from Table 2-4 that some of the coefficients were significant, with very small p-values (<0.05).

3. Effect of Various Parameters on Fluoride Removal Efficiency

The response surface plots of the second-order polynomial equations are given for significant two way interactions in Fig. 4. In these figures for showing the effect of each variable on the removal efficiency, one of them keeps at the central level and others vary within the determined experimental ranges.

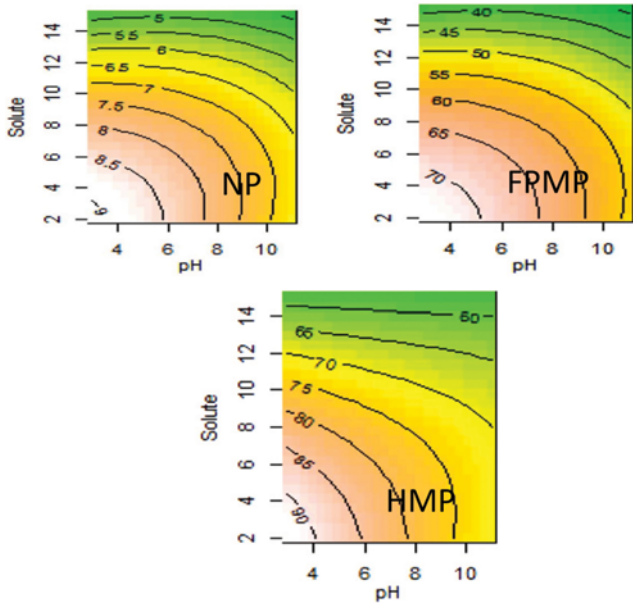

Fig. 4. Second-order response surface plot for fluoride removal (%).

3-1. Effect of pH

Based on Fig. 4 and negative values of pH coefficients in Eqs. (6)-(8), increasing pH led to decrease in fluoride removal efficiency. This finding may be due to the change in the surface charge of the adsorbent. The pH_{ZPC} values for NP, FEMP and HMP were 6.2. When the solution pH was below pH_{ZPC}, the fluoride anions were adsorbed to the positively charged surface of the adsorbents due to the electrostatic attraction. At pH above pH_{ZPC}, the surface of adsorbents was negatively charged and fluoride ions were repelled by them, resulting in the reduction of fluoride adsorption. Other studies have reported that removal efficiency increases with decreasing initial pH [18,37].

3-2. Effect of Initial Fluoride Concentration

Fig. 4 shows that fluoride removal efficiency decreases with an increase in fluoride concentration. This finding could be due to free sites on the adsorbent surface in lower initial fluoride concentrations.

3-3. Effect of Adsorbent Dosage

Based on Eqs. (6)-(8), the adsorbent dosage has the greatest regression coefficient and the greatest effect on fluoride removal. An increase in the adsorption with an increase adsorbent dosage can be attributed to a greater surface area and more available adsorption sites at higher adsorbent dosage. This result is in agreement with other studies [18,38].

4. Determining Optimal Settings

Based on the optimization results using the numerical method, the maximum efficiency was 9.39, 76.45, and 95.09% by NP, FEMP, and HMP, respectively at pH 3, adsorbent dosages 0.71, 0.75 and 0.70 g/L and fluoride initial concentration 2 mg/L.

5. Adsorption Kinetics

The kinetic experiments were carried out for different contact times at a constant adsorbent dosage (0.5 g/L), initial concentration (10 mg/L) and pH (7) agitated at 120 RPM. Then, the samples were taken at a programmed time interval. The fluoride adsorption was initially speeded up to 120, 60 and 60 min for NP, FEMP and HMP, respectively, and then slowed down. Thus, the optimum contact time was considered to be 120, 60 and 60 min for NP, FEMP and HMP, respectively. These times were used for further investigation. Two commonly used kinetic models were applied to analyze

Table 5. Kinetic parameters

Adsorbent	Pseudo-first-order kinetic					
	q_e (exp) (mg/g)	q_e (cal) (mg/g)	k_1	R^2	MPSD	HYBRID
NP	0.63	0.33	−0.034	0.8728	23.84	3.58
FEMP	7.96	4.13	−0.08	0.8893	24.02	45.96
HMP	8.34	4.26	−0.07	0.8664	24.46	49.96
Adsorbent	Pseudo-second-order kinetic					
	q_e (exp) (mg/g)	q_e (cal) (mg/g)	k_1	R^2	MPSD	HYBRID
NP	0.63	0.61	1.57	0.9991	1.61	0.01
FEMP	7.96	7.87	0.28	0.9994	0.55	0.02
HMP	8.34	8.2	0.29	0.9993	0.9	0.06

the adsorption data. The pseudo-first-order and pseudo-second-order models can be represented by Eqs. (9) and (10), respectively:

$$\ln(q_e - q_t) = \ln q_e - k_1 t \quad (9)$$

$$t/q_t = 1/k_2 q_e^2 + (t/q_e) \quad (10)$$

where q_e is the amount of fluoride adsorbed on the adsorbents at equilibrium conditions (mg/g) and q_t is the amount of fluoride adsorbed (mg/g) at any time represented by t (min), and k_1 and k_2 (mg/g·min) are the rate constants of pseudo-first-order and second-order models, respectively. According to the data in Table 5, the adsorption of fluoride on NP, FEMP and HMP was best described by the pseudo-second-order kinetic model (R^2>0.999). In addition, the calculated q_e values for pseudo-second-order kinetic model were similar to the experimental q_e values, indicated the efficiency of the fitted model (Fig. 5). Results were in agreement with most previous studies about the adsorption of fluoride on different adsorbents [10,14,18,29].

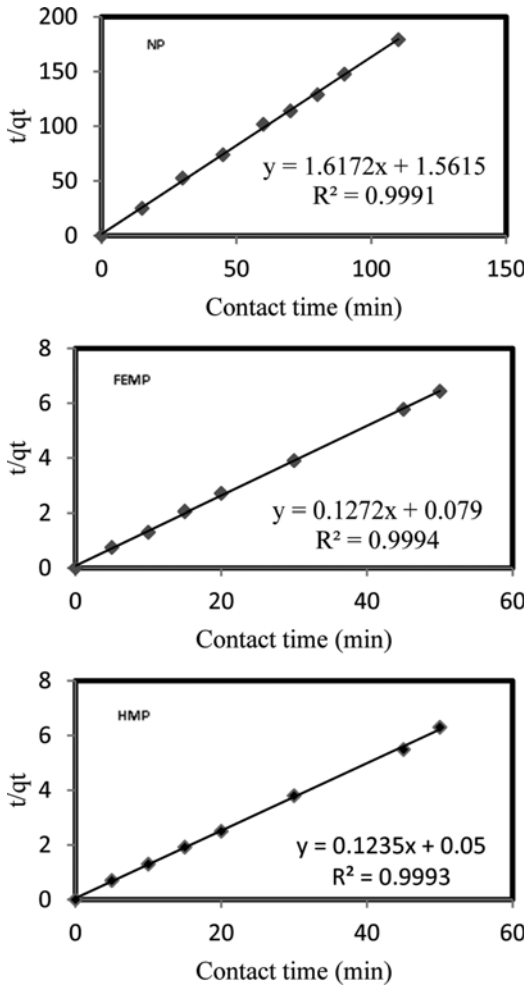

Fig. 5. Pseudo-second-order kinetic sorption of fluoride adsorption.

6. Adsorption Isotherms

Langmuir, Freundlich and Temkin models were used to express the relationship between the adsorbed fluoride ion on the adsorbent and the fluoride ion in the solution. The Langmuir model is expressed by Eq. (11):

$$q_e = q_m b C_e / 1 + b C_e \quad (11)$$

where C_e (mg/L) is the equilibrium concentration of the solute, q_e (mg/g) is the amount of solute per unit mass of the adsorbent, and q_m (mg/g) and b (L/mg) are Langmuir constants related to sorption capacity and rate of sorption, respectively. As summarized in Table 6, the maximum sorption capacity (q_m) for NP, FEMP, and HMP was 1.17, 21.74 and 25 mg/g, respectively, corresponding to an increase in the specific surface area 9.5, 24.5 and 31.5 m^2/g for NP, FEMP and HMP, respectively. This finding confirmed that the specific surface area was an important parameter in adsorption. Langmuir isotherm constant (b) depends on the adsorption energy and increases with the increase in adsorption bond potency [14]. The b values in this study for NP, FEMP and HMP were 0.36, 0.52 and 0.42, respectively. Thus, the adsorption bond was the maximum for FEMP and the minimum for NP. The affinity between fluoride and adsorbents can be predicted by using the Langmuir parameter b from the dimensionless separation factor R_L (Eq. (12)):

$$R_L = 1/1 + b C_0 \quad (12)$$

where C_0 and b are the initial fluoride concentration and Langmuir isotherm constant, respectively. The value of R_L represents the adsorption situations to be either unfavorable (R_L>1), linear (R_L= 1), favorable (0<R_L<1), or irreversible (R_L=0) [14]. The values of

Table 6. Isotherm parameters

Model	Adsorbent	R^2	k_f	n	MPSD	HYBRID
Freundlich	NP	0.9996	0.42	3.12	0.71	0.004
	FEMP	0.9991	8.13	2.56	1.15	0.130
	HMP	0.9970	8.13	2.08	2.24	0.530

Langmuir	Adsorbent	R^2	b	q_m	R_L	MPSD	HYBRID
	NP	0.9924	0.36	1.17	0.15-0.58	8.45	0.41
	FEMP	0.9952	0.52	21.74	0.11-0.27	4.59	2.23
	HMP	0.9951	0.42	25.00	0.13-0.29	3.11	1.35

Temkin	Adsorbent	R^2	k_T	B_T	MPSD	HYBRID
	NP	0.9888	4.78	0.23	3.98	0.10
	FEMP	0.9955	5.13	4.74	2.37	0.62
	HMP	0.9955	3.34	6.13	2.12	0.59

this parameter proved that fluoride situation with these adsorbents was favored under the conditions of this research (Table 6). The Freundlich model is expressed by the Eq. (13):

$$q_e=k_f C_e^{1/n} \quad (13)$$

where k_f and n are the indicators of adsorption capacity and adsorption intensity, respectively. The n value in the ranges of 2-10 indicates a favorable adsorption process [14]. Based on Table 6, the n value was in the range of 2-10, which represented a favorable adsorption process. The value of k_f increased after modification. Higher values of k_f indicated the higher sorption tendency by the adsorbent. The Temkin isotherm is represented by Eq. (14):

$$q_e=RT/bln(k_T C_e) \quad (14)$$

where k_T (L/g) is the binding constant that represents the maximum binding energy, $B_T=(RT)/b$ is the Temkin constant, R is the universal gas constant (8.314 J/mol·°k), and T is the absolute temperature in Kelvin. The constant b is related to the heat of adsorption [39].

According to the correlation coefficients, MPSD, and HYBRID in Table 6, the adsorption of fluoride on NP, FEMP and HMP correlated well with the Freundlich isotherm. Therefore, fluoride adsorption was multilayer that fluoride ion reacted first with adsorbent surface and then with each other on a heterogeneous surface of energy [40]. Comparative investigation of fluoride adsorption using NP, FEMP and HMP with other adsorbents is summarized in Table 7.

7. Thermodynamic Parameters

Thermodynamic parameters were evaluated by using the standard free energy change (ΔG), standard enthalpy change (ΔH^o), and standard entropy change (ΔS^o), and sticking probability (SP^*), given by Eqs. (15)-(19) and reported between 293 and 313 °K:

$$SP^*=(1-\beta)\exp-(E_a/RT) \quad (15)$$

$$\beta=1-C_e/C_0 \quad (16)$$

$$\ln K=-\Delta G/RT \quad (17)$$

$$K=q_e/C_e \quad (18)$$

$$\ln K=\Delta S^o/R-\Delta H^o/RT \quad (19)$$

where β is surface coverage, E_a is activation energy (kJ/mol), R is the gas law constant (8.314 J/mol·°K), T is the absolute temperature (°K), and K is sorption equilibrium constant. Generally, the value of activation energy specified the type of sorption, either physical (5-40 kJ/mol) or chemical (40-800 kJ/mol) [35]. Values of E_a (Table 8) suggested physical sorption with weak interactions (i.e., hydrogen bonding) between the fluoride ion and the adsorbent.

As seen in Table 8, the positive ΔG for NP in all temperatures suggested non-spontaneous adsorption, and negative for FEMP and HMP suggested spontaneous nature. This finding indicated that FEMP and HMP have a high affinity for the fluoride adsorption from the solution under experimental conditions. Furthermore, the positive values of ΔH^o and ΔS^o verified that the adsorption phenomenon was endothermic and random (at the solid/solution interface) during fluoride sorption [41]. Randomness is a motive force in the thermodynamic process. These results are in agreement with previous studies [14,18,29].

CONCLUSIONS

We have demonstrated that CCD with RSM can be applied to optimize the main experimental parameters for fluoride removal by using NP, FEMP, and HMP adsorbents. The experimental data complied with the second-order model. The optimum conditions were observed at pH=3, fluoride initial concentration=2 mg/L, and adsorption dosage=0.71, 0.75 and 0.70 g/L with the maximum efficiency 9.39, 76.45 and 95.09% for NP, FEMP and HMP, respectively. The pseudo-second order kinetic model had the best fit to the data. The equilibrium data were well fitted to the Freundlich model. The maximum sorption capacity was calculated 1.17, 21.74

Table 7. Comparative investigation of fluoride adsorption using NP, FEMP and HMP with other adsorbents

Adsorbent	Optimum pH	Kinetic model	Isotherm model	Capacity (mg/m)	Reference
Modified pumice with $MgCl_2$	6.00	Pseudo-second-order	Freundlich	5.50	[29]
Modified pumice with H_2O_2	6.00	Pseudo-second-order	Freundlich	11.76	[29]
Natural pumice	6.00	Pseudo-second-order	Freundlich	4.50	[29]
Modified pumice with HDTMA	6.00	Pseudo-second-order	Langmuir	41.00	[14]
Hydroxyapatite	4.16	Pseudo-second-order	Langmuir and Freundlich	3.12	[18]
Natural pumice	3.00	Pseudo-second-order	Freundlich	1.17	This study
Modified pumice with $FeCl_3$	3.00	Pseudo-second-order	Freundlich	21.74	This study
Modified pumice with HDTMA	3.00	Pseudo-second-order	Freundlich	25.00	This study

Table 8. Thermodynamic parameters

Adsorbent	E_a (kJ/mol)	ΔG					ΔS^o	ΔH^o
		293	298	303	308	313		
NP	2.03	4.81	4.81	4.77	4.72	4.68	0.007	6.92
FEMP	3.32	−4.82	−4.96	−5.19	−6.12	−6.63	0.090	23.16
HMP	2.26	−6.49	−6.79	−7.38	−7.81	−9.54	0.140	34.97

and 25 mg/g for NP, FEMP, and HMP, respectively. The adsorption process was physical with E_a values 2.03, 3.32, and 2.26 kJ/mol for NP, FEMP, and HMP, respectively. Positive ΔH^o and ΔS^o indicated an endothermic and random process. Positive ΔG for NP ascertained that the NP tendency for the fluoride removal was low and non-spontaneous, while negative ΔG for FEMP and HMP supported the feasibility of fluoride adsorption by them. This study demonstrated that FEMP and HMP had the adsorption capacity more than NP. Moreover, the adsorption capacity of HMP was higher than FEMP. Pumice is a natural and available adsorbent, but it has a low efficiency for the fluoride adsorption. Modification of pumice using $FeCl_3 \cdot 6H_2O$ and HDTM.Br cause a positive charge on its surface and the modified pumice is efficient for the fluoride adsorption.

ACKNOWLEDGEMENTS

This research has been supported by the Tehran University of Medical Sciences (90-03-27-14975). The authors are grateful to the Tehran University of Medical Sciences for its technical and financial support of this research.

ABBREVIATIONS

WHO : world health organization
RSM : response surface methodology
CCD : central composite design
NP : natural pumice
HDTM.Br : hexadecyl trimethyl ammonium bromide
FEMP : modified pumice
HMP : HDTM.Br modified pumice
FESEM : field emission scanning electron microscope
XRD : X-ray diffraction
XRF : X-ray fluorescence
FTIR : fourier transform infrared spectroscopy
BET : brunauer emmett-teller
pH_{ZPC} : pH of the zero point charge
MPSD : Marquardt's percent standard deviation
HYBRID : hybrid error functions
BJH : Barrett-Joyner-Halenda
ANOVA : analysis of variance
ΔG : free energy change
ΔH^o : standard enthalpy change
ΔS^o : standard entropy change
SP^* : sticking probability

Symbols

β : beta
Δ : delta
Σ : sigma

REFERENCES

1. D. R. Lide, *Crc handbook of chemistry and physics*, CRC Press (2004).
2. WHO, *Guidelines for drinking-water quality*, World Health Organization (2011).
3. M. Islam and R. Patel, *Chem. Eng. J.*, **169**, 68 (2011).
4. S. Ghorai and K. K. Pant, *Sep. Purif. Technol.*, **42**, 265 (2005).
5. K. Hu and J. M. Dickson, *J. Membr. Sci.*, **279**, 529 (2006).
6. D. Ghosh, C. R. Medhi and M. K. Purkait, *Chemosphere*, **73**, 1393 (2008).
7. P. Sehn, *Desalination*, **223**, 73 (2008).
8. N. Viswanathan and S. Meenakshi, *J. Hazard. Mater.*, **162**, 920 (2009).
9. L. A. Richards, M. Vuachère and A. Schäfer, *Desalination*, **261**, 331 (2010).
10. T. Zhang, H. Yu, Y. Zhou, J. Rong, Z. Mei and F. Qiu, *Korean J. Chem. Eng.*, **33**, 720 (2016).
11. R. Buamah, C. A. Oduro and M. H. Sadik, *J. Environ. Chem. Eng.*, **4**, 250 (2016).
12. Y. Zhang, D. Wang, B. Liu, X. Gao, W. Xu, P. Liang and Y. Xu, *Am. J. Anal. Chem.*, **4**, 48 (2013).
13. M. Kitis, S. Kaplan, E. Karakaya, N. Yigit and G. Civelekoglu, *Chemosphere*, **66**, 130 (2007).
14. Gh. Asgari, B. Roshani and Gh. Ghanizadeh, *J. Hazard. Mater.*, **217**, 123 (2012).
15. J. P. Wang, Y. Z. Chen, X. W. Ge and H. Q. Yu, *Colloids Surf., A.*, **302**, 204 (2007).
16. R. H. Myers, D. C. Montgomery and C. M. Anderson-Cook, *Response surface methodology: Process and product optimization using designed experiments*, John Wiley & Sons (2016).
17. K. Yaghmaeian, S. Silva Martinez, M. Hoseini and H. Amiri, *Desalin. Water Treat.*, **57**, 57 (2016).
18. M. Mourabet, A. El Rhilassi, H. El Boujaady, M. Bennani-Ziatni, R. El Hamri and A. Taitai, *J. Saudi Chem. Soc.*, **19**, 603 (2015).
19. A. Hassani, R. Darvishi Cheshmeh Soltani, M. Kıranşan, S. Karaca, C. Karaca and A. Khataee, *Korean J. Chem. Eng.*, **33**, 178 (2016).
20. J. D. Cui, *Korean J. Chem. Eng.*, **27**, 174 (2010).
21. T. Tshukudu, H. Zheng, X. Hua, J. Yang, M. Tan, J. Ma, Y. Sun and G. Zhu, *Korean J. Chem. Eng.*, **30**, 649 (2013).
22. J. Órfão, A. Silva, J. Pereira, S. Barata, I. Fonseca, P. Faria and M. Pereira, *J. Colloid Interface Sci.*, **296**, 480 (2006).
23. R Core Team, A Language and Environment for Statistical Computing and R Foundation for Statistical Computing, Vienna, Austria (2015). Available from: <http://www.r-project.org/>.
24. R. V. Lenth, *J. Stat. Software*, **32**, 1 (2009).
25. APHA, AWWA and WEF, *Standard methods for the examination of water and wastewater*, American Public Health Association (2005).
26. Gh. Ghanizadeh and Gh. Asgari, *React. Kinet. Mech. Cat.*, **102**, 127 (2011).
27. S. Wang and Z. Zhu, *J. Hazard. Mater.*, **136**, 946 (2006).
28. M. Li, X. Zhu, F. Zhu, G. Ren, G. Cao and L. Song, *Desalination*, **271**, 295 (2011).
29. M. Noori Sepehr, V. Sivasankar, M. Zarrabi and M. S. Kumar, *Chem. Eng. J.*, **228**, 192 (2013).
30. M. R. Samarghandi, M. Zarrabi, A. Amrane, M. M. Soori and M. Noori Sepehr, *Environ. Eng. Manage. J.*, **12**, 2137 (2013).
31. M. Malakootian, M. Moosazadeh, N. Yousefi and A. Fatehizadeh, *Afr. J. Environ. Sci. Technol.*, **5**, 299 (2011).
32. M. Noori Sepehr, M. Zarrabi, H. Kazemian, A. Amrane, K. Yaghmaian and H. R. Ghaffari, *Appl. Surf. Sci.*, **274**, 295 (2013).
33. R. E. Grim, *Clay mineralogy*, McGraw-Hill Book Compony (1968).
34. H. Yamada, S. Yokoyama, Y. Watanabe, H. Uno and K. Tamura,

Sci. Technol. Adv. Mater., **6**, 394 (2005).
35. J. R. Stevens, R. V. Siriwardane and J. Logan, *Energy Fuels*, **22**, 3070 (2008).
36. H. Naeimi, A. Mohajeri, L. Moradi and A. Rashidi, *Appl. Surf. Sci.*, **256**, 631 (2009).
37. H. Nourmoradi, A. Ebrahimi, Y. Hajizadeh, S. Nemati and A. Mohammadi, *Int. J. Pharm. Technol.*, **8**, 13337 (2016).
38. M. Faraji, E. Abooi Mehrizi, M. Sadani, M. Karimaei, E. Ghahramani, K. Ghadiri and M. S. Taghizadeh, *Int. J. Environ. Health Eng.*, **1**, 26 (2012).
39. A. El Nemr, *J. Hazard. Mater.*, **161**, 132 (2009).
40. R. Arasteh, M. Masoumi, A.M. Rashidi, L. Moradi, V. Samimi and S. T. Mostafavi, *Appl. Surf. Sci.*, **256**, 4447 (2010).
41. C. S. Sundaram, N. Viswanathan and S. Meenakshi, *J. Hazard. Mater.*, **155**, 206 (2008).